H⁻ TEMPERATURE MEASUREMENTS BY A SLIT DIAGNOSTIC TECHNIQUE*

Joseph D. Sherman, H. Vernon Smith, Jr., Carl Geisik, and Paul Allison
Los Alamos National Laboratory
Los Alamos, NM 87545

Abstract

H^- ion beams are extracted at 5-25 kV from a long, narrow slit on a Penning surface-plasma source (the 8X source). The extraction geometry produces negligible transverse electric fields (focusing effects) along the slit length. Therefore, the ion angular spread reflects the distribution of ion energies at the plasma surface. The angular distributions are measured with an electric-sweep emittance scanner whose slits are oriented normal to the long dimension of the emission slit. The nearly Maxwellian angular distributions measured over the central portions of the ribbon beam give kT_{H^-} of 0.1 to 0.2 eV for a 2-A dc discharge and 0.8 to 1.0 eV for 350- to 500-A pulsed discharges. This diagnostic technique has sufficient position resolution to allow measurement of the kT_{H^-} spatial distributions. It also allows study of the kT_{H^-} dependencies on ion source parameters (e.g., increasing the H_2 gas flow lowers kT_{H^-}).

I. INTRODUCTION

One mechanism proposed for H^- production in the Penning surface-plasma source (SPS) is the resonant charge exchange of fast cathode (≈100 eV) H^- with lower energy (≈1 eV) H^o atoms within the plasma discharge [1]. If this production mechanism dominates, then the fast H^- ions equilibrate to the H^o temperature before extraction. Previous measurements by spectroscopic methods [2,3] in SPS sources show that the H^o temperature is one eV, so an intrinsic kT_{H^-} of this order may be expected. Measurements of kT_{H^-} in ion-source plasmas by laser diagnostic techniques have been initiated [4]. In the present experiment, we use a method based on ion-optical considerations and the use of an emittance-measuring device [5] to determine kT_{H^-}.

By measuring the angular distribution of H^- ions extracted from the central region of a long, narrow emission slit, the slit-end aberrations and other focusing effects may be neglected. The measured angle θ is then related to the ion thermal energy $\phi_\perp$ and the beam energy ϕ_b by $\theta = \sqrt{\phi_\perp/\phi_b}$. The cathode-cathode and anode-anode gaps within the 8X source [6] are both 3.40 cm. These dimensions allow installation of a long emission slit from which a H^- beam may be extracted. Using a Maxwellian model for the distribution function $f(\theta) = \exp(-\theta^2 \phi_b/kT_{H^-})$ gives

$$kT_{H^-} = 0.361\ \phi_b\ (\theta_{FWHM})^2 \qquad (1)$$

for the inherent kT_{H^-} in the source plasma, where θ_{FWHM} is determined from the measured beam angular distributions.

* Work supported by the Dept. of Defense, US Army Strategic Defense Command under auspices of the US Dept. of Energy.

II. EXPERIMENTAL METHOD

A slit emitter ℓ_e = 3.66 cm long and 0.061 cm wide is constructed for the 8X source. The extractor slit is 3.9 cm long and 0.086 cm wide. The extraction system allows the emitting plasma to be examined in either the cathode-to-cathode (parallel to the magnetic field) or anode-to-anode (perpendicular to the magnetic field) directions. The emission and extraction slits are parallel to within ≈5 mrad. The extraction gap in these experiments is 0.49 cm.

Figure 1 is a schematic of the experimental arrangement with the anode-to-anode orientation of the slit extraction system. The "y" scanner is used to measure the H^- angular distributions as a function of position. The electric-sweep scanner (ESS) [5] entrance slit is located d = 12.3 cm from the plasma emitter. The ESS analyzing slits are oriented perpendicular to the long dimension of the emission slit. Maximum scanner angular acceptance θ_{scan} = ±142 mrad, so the observable length at the emitter position is ℓ_s = $2d \tan(\theta_{scan})$ = 3.52 cm. This distance is about the same as the emitter length ℓ_e. To separate the thermal group of ions from those from the slit ends, $\ell_e >> 2d\sqrt{(kT/\phi_b)} \approx 0.2$ cm is required and easily satisfied here. Beam space-charge is neutralized beyond the 0.49-cm extraction gap by positive ions produced by beam-ionization of the background gas [7]. The scanner angular resolution is ±0.5 mrad, so the energy resolution at 20 keV beam energy is ≈0.002 eV.

The y-plane, 15-kV phase-space diagram shown in Fig. 2 for a discharge current i_d = 350 A consists of 50 position slices. The angle full scale on this plot is ±39.6 mrad. At the extreme positions, large beam aberrations that correspond to ion extraction at the slit ends are observed. The predominant

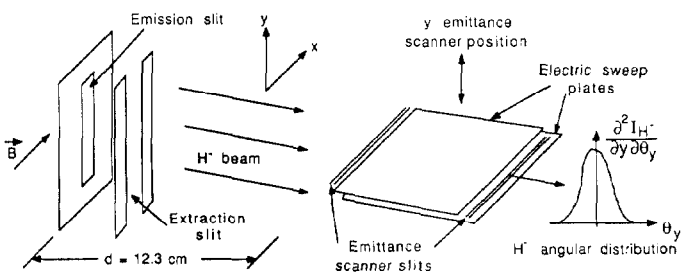

Fig. 1. The experimental arrangement for the kT_{H^-} measurements. The emitter is in the anode-to-anode configuration (perpendicular to the magnetic field), where the magnetic field is along the x direction. The ESS slits are orthogonal to the emission and extraction slits.

0-7803-0135-8/91$01.00 ©IEEE

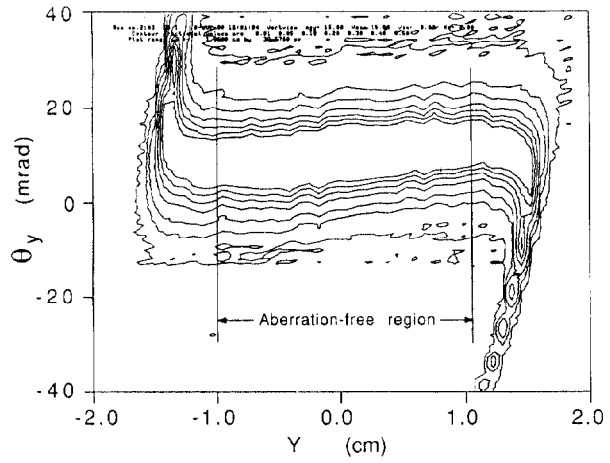

Fig. 2. Phase-space diagram for a y-plane emittance scan (anode-to-anode orientation of the emission slit) at 15 kV.

feature of the scanned beam in the central portion is the angular width caused by the thermal energy of the H^- ions. The central region of the beam has a small envelope divergence, λ = 1.8 mrad/cm. Figure 3 shows the beam current oscillogram at 1-MHz bandwidth for the phase-space diagram shown in Fig. 2. The Faraday cup is not large enough to capture the whole beam, so the H^- current should be multiplied by ≈1.5 to obtain the full beam current. The approximate emission current density is 230 mA/cm^2 for i_d = 350 A, 1 mA/cm^2 for i_d = 2A. The 8X source is tuned to obtain good beam quiescence. The ESS ramp voltage is superimposed on Fig. 3; the angular distribution data are acquired between 1.6 and 1.9 ms.

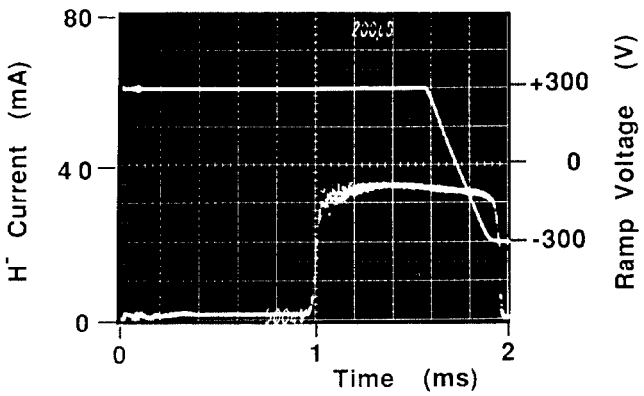

Fig. 3. Oscillogram showing the H^- beam current and the ESS ramp voltage.

The angular distribution in the x- (or narrow-) plane may be large, dominated by focusing effects. If the emission slit and the emittance scanner slits are misaligned by angle α, then $\delta\theta y/\theta y \approx (\alpha^2/2)[(\theta x/\theta y)^2 - 1]$, where θ_x and θy are rms angles. For our measured conditions of $\theta x/\theta y \approx 5$ and $\alpha < 30$ mrad, the error is ≈1%. For cathode-cathode slit orientation, a similar conclusion is reached.

III. RESULTS AND DISCUSSION

The angular distribution data for a position slice near the center of the Fig. 2 emittance scan (pulsed discharge) is shown in Fig. 4. A Maxwellian fit to the data with a least-squares fitting routine gives kT_{H^-} = 0.81 eV from equation 1. Also shown in Fig. 4 is one sample of the 2-A dc-discharge data with a fit of kT_{H^-} = 0.18 eV. The peak amplitude of the dc data has been normalized to the pulsed data in Fig. 4.

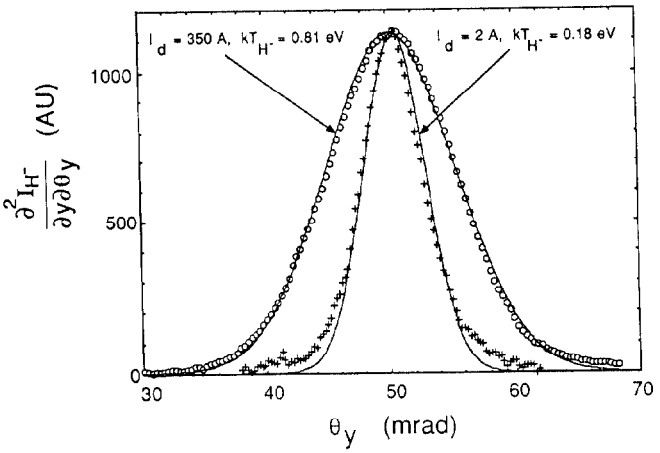

Fig. 4. Typical Maxwellian fits to angular distributions for pulsed and dc discharges. Both measurements are made at y = 0.04 cm, near the discharge center.

Because the beam is slightly diverging ($\lambda > 0$), the angles at the analyzer will be reduced by $\delta\theta/\theta = -\lambda d = -0.023$, which amounts to about 0.05 eV for the pulsed discharge. The observed divergence (positive) is consistent with weak beam-space-charge expansion in the accel gap. Data analysis of several phase-space plots shows that the divergence correction to kT_{H^-} increases with the beam perveance, and in all cases the correction is less than 5%.

The approximate uncertainties in the measurement presented here in terms of their effects on kT are (1) beam energy—2%, (2) ESS design calibration—1%, (3) digitization—1%, (4) fit routine—2%, (5) space charge—5%, (6) alignment accuracy—1%, so overall accuracy should be ≈6%.

An estimate for the plasma surface length ℓ_p which contributes to the angular distribution for the pulsed discharge in Fig. 4 is $\ell_p = 2d \tan(\theta_{FWHM}/2) = 0.15$ cm $<< \ell_s$. This result shows that the kT_{H^-} may be obtained as a function of position along the emission slit. Temperatures are derived from the measured H^- angular distributions at about thirty of the fifty positions (0.08 cm step size). The derived kT_{H^-} vs position for the Fig. 2 diagram is shown in Fig. 5a. The

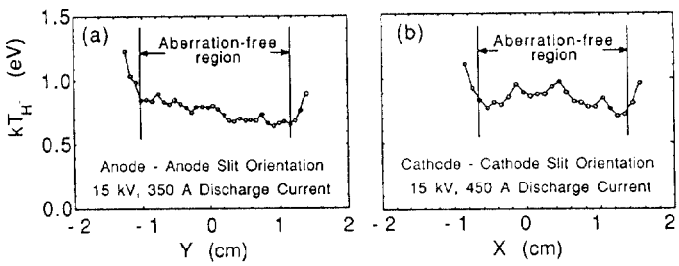

Fig. 5. Measured kT_{H^-} as a function of scanner position.

emitter is in the anode - anode orientation, perpendicular to the magnetic field. The apparent temperature rise at the ±1 cm positions is caused by the onset of significant transverse electric fields. A gradual decrease in the kT_{H^-} is noted with position increase over the central portion in Fig. 5a. This may be caused by increased gas density since the H_2 gas feed is located at y = +1.7 cm in the discharge chamber. Figure 5b shows the kT_{H^-} as a function of position for the cathode-cathode orientation, parallel to the magnetic field. There is no large systematic variation of temperatures with position in Fig. 5b.

Measurements of kT_{H^-} as a function of ϕ_b, for the anode-anode orientation are shown in Fig. 6 for (a) a dc discharge at 2 A and (b) a pulsed discharge at 470 A. Here the H^- temperature has been averaged over all the positions where slit-end aberrations are not present. The derived temperatures are independent of the beam perveance or energy, as they must be for a true temperature. Temperatures for the dc discharges are 0.1 - 0.2 eV (cf. Fig. 4), whereas those for the pulsed measurements are 0.8 - 1.0 eV. Lower discharge currents produce lower H^- ion temperatures just as they produce lower H^0 temperatures [2,3].

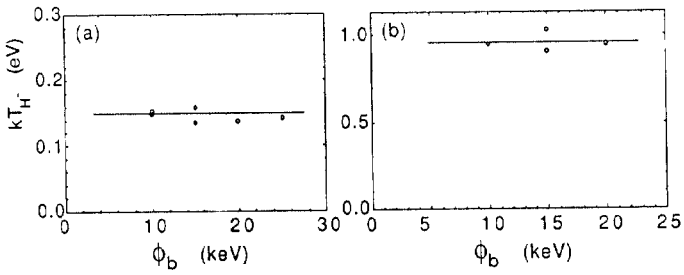

Fig. 6. Measured kT_{H^-} as a function of the beam energy for (a) a 2-A dc discharge and (b) a 470-A pulsed discharge. Constant temperature lines are shown to guide the eye.

Parametric dependencies of kT_{H^-} on the 8X ion source operating parameters are measured. These include H_2 gas flow, discharge current (pulsed and dc), extraction voltage, plasma position along the slit, and emission slit orientation. The kT_{H^-} (averaged over the aberration-free region) is plotted vs the H_2 gas flow for the anode-anode and cathode-cathode slit orientations in Figs. 7a and 7b. Both data sets show the same behavior: kT_{H^-} decreases with increasing H_2 gas flow. No significant dependence of kT_{H^-} on magnetic-field orientation is observed.

IV. SUMMARY

Temperature measurement of the H^- ions is made by analyzing the angular distribution of ions extracted from a long slit. The plasma generator must be large enough to install a sufficiently long slit to separate the thermal ions from the slit-end ions at the analyzer and to minimize space-charge effects. We assume

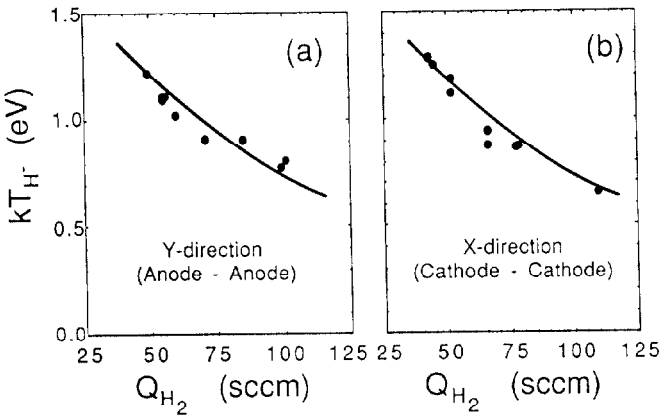

Fig. 7. Plots of kT_{H^-} vs H_2 gas flow for the (a) anode-anode and (b) cathode-cathode slit orientations. Identical guide-to-the-eye curves are shown on both plots.

that for the 8X Penning SPS the angular spread in the beam central region is dominated by the plasma H^- ion temperature. The envelope divergence at the analyzer is small, showing that the beam space-charge expansion in the extraction gap is small. A result of these measurements is that the inherent H^- ion temperature for the Penning SPS source may be considerably lower than previous estimates [3] and close to the previously measured H^0 temperatures. Those measurements suggest an intimate link between the H^0 and H^- species in this plasma.

V. ACKNOWLEDGMENT

The authors thank David R. Schmitt for his experimental assistance.

VI. REFERENCES

[1] G. E. Derevyankin and V. G. Dudnikov, AIP Conf. Proc. No. 111, p. 376 (1984).

[2] H. V. Smith, Jr., P. Allison, E. J. Pitcher, R. R. Stevens, Jr., G. T. Worth, G. C. Stutzin, A. T. Young, A. S. Schlachter, K. N. Leung, and W. B. Kunkel, Rev. Sci. Instrum. 61 , 424 (1990), and AIP Conf. Proc. No. 210, 462 (1990).

[3] H. V. Smith, Jr., P. Allison, and R. Keller, AIP Conf. Proc. No. 158, 181 (1987).

[4] P. Devynck, J. Auvray, M. Bacal, P. Berlemont, J. Bruneteau, R. Leroy, and R. A. Stern, Rev. Sci. Instrum. 60 , 2873 (1989).

[5] P. W. Allison, J. D. Sherman, and D. B. Holtkamp, IEEE Trans. Nuc. Sci. NS-30, 2204 (1983).

[6] H. V. Smith, P. Allison, K. Saadatmand, and J. D. Schneider, Proc. Second European Particle Accelerator Conf. (Editions Frontieres, Gif-sur-Yvette, 1990) p. 659.

[7] J. Sherman, E. Pitcher, and P. Allison, 1988 Linear Accelerator Conf. Proc., CEBAF-REPORT-89-001, p. 155-157, and Rev. Sci. Instrum. 61, 616 (1990).